

Molecular Dynamics Study of Conformations of Beta-Cyclodextrin and its Eight Derivatives in Four Different Solvents

Wasinee Khuntawee^{1,2,3}, Mikko Karttunen⁴, and Jirasak Wong-ekkabut^{1,2,3,*}

¹Department of Physics, Faculty of Science, Kasetsart University, Bangkok 10900, Thailand

²Computational Biomodelling Laboratory for Agricultural Science and Technology

(CBLAST), Faculty of Science, Kasetsart University, Bangkok 10900, Thailand

³Thailand Center of Excellence in Physics (ThEP Center), Commission on Higher Education, Bangkok 10400, Thailand

⁴Department of Chemistry and Department of Applied Mathematics, Western University, 1151 Richmond Street, London, Ontario N6A 5B7, Canada

*E-mail addresses: jirasak.w@ku.ac.th (J. Wong-ekkabut)

Abstract

Understanding the atomic level interactions and the resulting structural characteristics is required for developing beta-cyclodextrin (β CD) derivatives for pharmaceutical and other applications. The effect of four different solvents on the structures of the native β CD and its hydrophilic (methylated β CD; ME β CD and hydroxypropyl β CD; HP β CD) and hydrophobic derivatives (ethylated β CD; ET β CD) were explored using molecular dynamics (MD) simulations and solvation free energy calculations. The native β CD, 2-ME β CD, 6-ME β CD, 2,6-DM β CD, 2,3,6-TM β CD, 6-HP β CD, 2,6-HP β CD and 2,6-ET β CD in non-polar solvents (cyclohexane; CHX and octane; OCT) were stably formed in symmetric cyclic cavity shape through their intramolecular hydrogen bonds. In contrast, β CDs in polar solvents (methanol; MeOH and water; WAT) exhibited large structural changes and fluctuations leading to significant deformations of their cavities. Hydrogen bonding with polar solvents was found to be one of the major contributors to this behavior: solvent- β CD hydrogen bonding strongly competes with intramolecular bonding leading to significant changes in structural stability of β CDs. The exception to this is the hydrophobic 2,6-ET β CD which retained its spherical cavity in all solvents. Based on this, it is proposed that 2,6-ET β CD can act as a sustained release drug carrier.

Keywords: Methylated beta-cyclodextrin, Ethylated beta-cyclodextrin, Hydroxypropyl beta-cyclodextrin, Molecular dynamics simulations, Solvation effects

1. Introduction

Cyclodextrins (CDs) are cyclic oligosaccharides (ring-structured sugar compounds) commonly used in pharmaceutical and food industry for drug complexes and improved solubility, and as cholesterol removers, respectively.^{1, 2} Perhaps the most famous application of CDs, however, is in the commercial odor remover Febreze in which CDs are used to capture “stinky” molecules.³ Three of CDs, alpha CD (α CD), beta CD (β CD) and gamma CD (γ CD), are naturally occurring and consist of α -(1,4) linked D-glucopyranose with six, seven or eight units, respectively. The general shape of all CDs is a truncated cone with hydrophilic outer surface and hydrophobic interior, Figure 1. Cyclodextrins’ history, development and applications have been recently reviewed by Crini.⁴

In this work, we use molecular dynamics (MD) simulations and solvation free energy calculations to investigate conformational properties of the native β CD, four derivatives of methylated β CD (ME β CD), three derivatives of hydroxypropyl β CD (HP β CD), and one ethylated β CD (ET β CD) derivative. ET β CD is hydrophobic⁵ while all the rest are hydrophilic. These systems were studied in four different solvents, cyclohexane (CHX), methanol (MeOH), octane (OCT) and water (WAT). The list of all systems is provided in Table 1. This focus is primarily motivated by the fact that in pharmaceutical applications, renal side effects have been reported for parenteral administration and suggested to be a result of poor water solubility.^{6, 7} Despite previous studies regarding water solubility⁸⁻¹¹, complex stability^{12, 13}, bioavailability of β CD inclusion complexes^{10, 14, 15}, and improvements by substitutions of the hydroxyl groups with various functional groups, the molecular origin of these effects is not known.

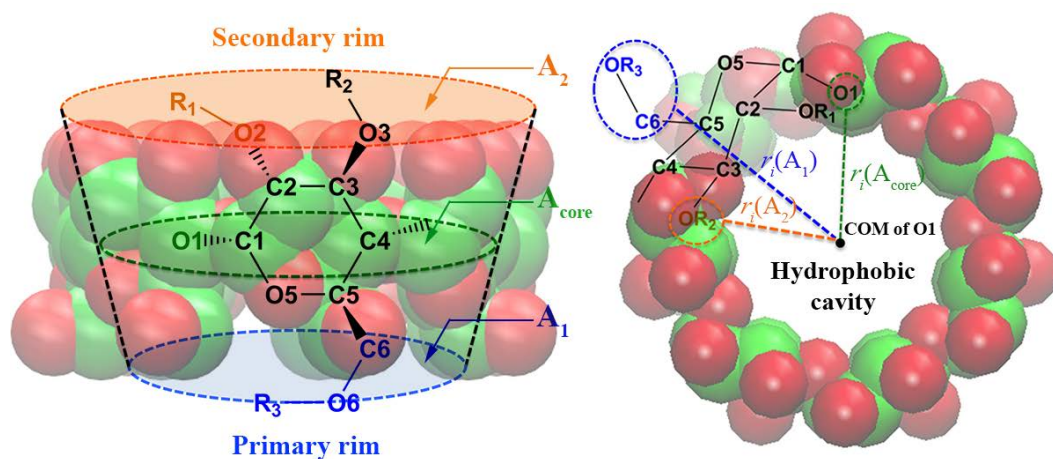


Figure 1: Left: Side-view of native β CD forming a truncated cone, showing the glucose subunit and atom name labeling. The rim at C6 is called the primary rim with the associated area A_1 , while the opposite

rim, consisting of C2 and C3 is the secondary rim (area A_2). A_{core} denotes the area at the center of the cavity. The R groups are varied for the β CD derivatives. R_1 , R_2 and R_3 of all seven glucose subunits of the native β CD are hydrogen atoms. For the derivatives, R_1 , R_2 or R_3 of are replaced by methyl ($-\text{CH}_3$), 2-hydroxypropyl ($-\text{CH}_2\text{CH}(\text{OH})\text{CH}_3$) and ethyl ($-\text{CH}_2\text{CH}_3$) group, called methylated β CD, hydroxypropyl β CD and ethylated β CD, respectively. Right: Top-view of the β CD showing its hydrophobic cavity. The red and green spheres represent oxygen and carbon atoms, respectively. Hydrogen atoms are omitted for clarity.

Different functionalizations have been reported to alter structural, physicochemical and biological properties of β CDs.^{16, 17} In addition, structural studies of several β CD types using X-ray diffraction and computer simulations have been conducted.¹⁸⁻²² As a particular feature, Li et al.²³ found that the crystal structure of the native β CD is a truncated cone due to intramolecular hydrogen bonds (H-bonds) between the R_1 and R_2 groups of adjacent glucose subunits (Figure 1). Substitutions by methyl groups at R_1 and R_3 , (Figure 1) called 2,6-dimethylated- β -CD (2,6-DM β CD; the numbers correspond to the numbering of the oxygen atom linking to those functional groups) narrowed the primary rim but the cavity still retained its cyclic shape due to intramolecular H-bonds.²⁴

Structural characterization of β CD derivatives requires their synthesis which is rather difficult since substitutions at R_1 , R_2 and R_3 compete with each other (Figure 1).¹⁸ Computer simulations offer an alternative approach to study structure and conformational changes. For example, Yong et al.²² used MD simulations to study the structural properties of HP β CD derivatives with varying numbers and positions of substituent groups in water. They found that structural changes in cavity shapes influence their interactions with guest ligands and the surrounding solvents and intra-molecular interactions. In another MD study, the rate constant for hydrogen bond breaking and reformation between β CDs and water around/inside cavity was observed to decrease for ME β CDs in comparison to the native β CD.²⁵

Previous experiments have shown that water solubility of ME β CD and HP β CD can be enhanced by over 20-fold, compared to the native β CD.²⁶⁻²⁹ In contrast, the solubility of ET β CD is three orders of magnitudes lower than that of the native β CD.^{5, 30} This change in solubility most likely results from changes in intramolecular hydrogen bonding and hydrogen bonds with water. It has been shown, that toxicity depends on the number of functional groups and their positions³¹ and that in drug delivery systems modified hydrophilicity due to substitutions results in different drug release profiles. In particular, hydrophilic β CD derivatives (see Table 1) can be used as immediate release transporters via increasing dissolution rate and adsorption of poorly water-soluble drugs, whereas hydrophobic derivatives act as sustained release drug carriers for water-soluble compounds.³² Recent results also show that most poorly water-soluble drugs bind strongly to ME β CD and HP β CD derivatives which leads to a significant

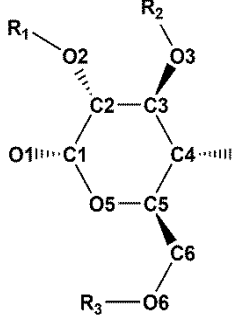
increase in solubility compared to free drugs as well as drugs complexed with the native β CD.¹⁷ Several studies have also suggested that this improvement might be a result from changes in shape and solvent interactions of β CD derivatives^{33, 34}; combination of CD complexation and co-solvation is one of the most promising techniques for improvement of drug solubility.^{26, 34} Using alcohols (e.g. methanol, ethanol, etc.) as co-solvents, water solubility of guest ligands has been shown to increase.³⁵ The addition of non-polar solvent may also enhance the binding affinity of the guest ligand to the β CD's cavity.³⁶ Moreover, non-polar solvents have an important role in the purification process of CDs. In particular, cyclohexane helps to separate CDs from non-converted starch.³⁷ The precise molecular level mechanisms remain unresolved and thus detailed structural analyses are fundamental to understanding β CDs' properties. Resolving them is the aim of this paper.

2. Methodology

2.1) System preparation

Structural properties of the native β CD and its derivatives (ME β CD, HP β CD and ET β CD) were investigated in four different solvents (water, methanol, octane and cyclohexane) by atomistic MD simulations. The initial β CD configuration was taken from a previously relaxed β CD.³⁸ The starting structures of the derivatives were prepared from the native structure in which the hydrogen atoms of the hydroxyl groups at carbon positions 2-, 6-, 2,6- and 2,3,6- for all seven glucoses subunits were replaced by methyl groups, 2-hydroxypropyl groups and ethyl groups for β CD derivatives of ME β CD, HP β CD and ET β CD, respectively. The native β CD and eight different β CD derivatives are described in Table 1.

Table 1: Details of native β CD and its derivatives. The derivatives are classified into two main groups: 1) hydrophilic (ME β CDs and HP β CDs) and 2) hydrophobic (ET β CD) according to their water solubility with respect to the native β CD. The position and number of functional groups were varied for ME β CDs and HP β CDs. The number in the name of each β CD derivative corresponds to the number of oxygen atom connecting to the functional group R. The functional groups were fully substituted for all seven glucose subunits.

				
Model	System	R ₁	R ₂	R ₃
a) Native β CD				
1	β CD	-H	-H	-H
Hydrophilic β CDs				
b) Methylated β CD derivatives				
2	2-ME β CD	-CH ₃	-H	-H
3	6-ME β CD	-H	-H	-CH ₃
4	2,6-DM β CD	-CH ₃	-H	-CH ₃
5	2,3,6-TM β CD	-CH ₃	-CH ₃	-CH ₃
c) Hydroxypropyl β CD derivatives				
6	2-HP β CD	-CH ₂ CH(OH)CH ₃	-H	-H
7	6-HP β CD	-H	-H	-CH ₂ CH(OH)CH ₃
8	2,6-HP β CD	-CH ₂ CH(OH)CH ₃	-H	-CH ₂ CH(OH)CH ₃
Hydrophobic β CDs				
d) Ethylated β CD derivative				
9	2,6-ET β CD	-CH ₂ CH ₃	-H	-CH ₂ CH ₃

The GROMACS 5.1.1 package³⁹ was used to perform the MD simulations. The molecular models of native β CD, β CD derivatives, methanol, octane and cyclohexane were represented by the Gromos53a6 force field;^{40, 41} we also tested the native β CD system with GLYCAM06 force field⁴² and the results were similar. The partial charges and atom types of substituent groups in M β CD, HP β CD and ET β CD are shown in Figure S1. In simulations, the β CD in question was initially positioned at the center of the simulation box and fully solvated with 7000 single point charge (SPC) water molecules⁴³, 1728 methanol molecules, 1000 octane molecules or 2000 cyclohexane molecules depending on the solvent. The details of the simulated systems are shown in Table S1.

2.2) MD simulations

All initial structures were first energy minimized by using the steepest descent algorithm. This was followed by an MD simulation with a time step of 2 fs in the NPT (constant particle number, pressure and temperature) ensemble. The root mean square displacement (rmsd) of all atoms in the β CD molecules relative to their minimized structures was monitored and it was determined that the systems had reached equilibrium after 70 ns (Figure S2). Data collection for analysis started after that. The total simulation time for each of the systems was 100 ns. The Lennard-Jones and the real-space part of electrostatic interactions were cut-off at 1.0 nm. For long-range electrostatic interactions, the particle-mesh Ewald (PME) method⁴⁴⁻⁴⁶ was used with the reciprocal-space interactions evaluated on a 0.12 nm grid with cubic interpolation of order four. The P-LINCS algorithm was used to constrain all bond lengths.⁴⁷ Isotropic pressure coupling was applied using the Berendsen algorithm⁴⁸ at 1 bar with a time constant of 3.0 ps and compressibility of $4.5 \times 10^{-5} \text{ bar}^{-1}$. The Parrinello-Donadio-Bussi velocity rescale thermostat algorithm was applied independently for β CD and water at 298 K.^{49, 50} Periodic boundary conditions were applied in all directions. The above simulation protocol has been previously validated and used for several lipid and protein systems, for recent ones, see e.g. Refs.⁵¹⁻⁵⁴. The Visual Molecular Dynamics (VMD) software was used for all molecular visualizations.⁵⁵

3. Results and discussions

3.1) Structural changes in solvents

Structural changes from the energy-minimized structure were measured by the root mean square displacement (rmsd) for all atoms in the β CDs. Figures 2(a)-(i) show the rmsd distributions in different solvents. The averages rmsd are shown in Table S2. Fluctuations of the rmsd distributions can be discussed in terms of the full width at half maximum (FWHM) of the RMSD distributions, as shown in Table S3. The distributions were fitted to a Gaussian model and the FWHM values were calculated using

$FWHM = 2\sqrt{\ln 4} \cdot \sigma$ where σ is the standard deviation. In general, FWHM was lower in non-polar solvents than in polar ones with the following exceptions: 2,3,6-TM β CD in OCT, 2-HP β CD in OCT, 6-HP β CD in OCT and 2,6-ET β CD in CHX and OCT. Interestingly, the FWHM of the hydrophobic 2,6-ET β CD in polar solvents is smaller than in non-polar solvent. This is in contrast to the hydrophilic derivatives as 2,6-DM β CD and 2,6-HP β CD which have their substituent groups at the same positions.

The rmsd of the native β CD peaks around 0.11 nm in OCT, and around 0.12 nm, 0.20 nm and 0.26 nm in CHX, MeOH and WAT, respectively (Figure 2(a) and Table S2). The rmsd value of the native β CD in water is similar to the previous MD simulation using the same force field as us (Gromos53a6)⁵⁶; the general β CD structural properties using Gromos53a6 are in agreement with X-ray scattering and simulations with other force fields^{42, 57}. Compared to the native β CD in water, the rmsd peak position was about 23% smaller in MeOH. This tendency has been reported in previous simulations^{21, 58}, but the difference in their results was smaller by about 17%⁵⁸. This may be due the difference in simulation times and solvation: our simulations were performed at higher solvation level and are an order of magnitude longer (10 vs 100 ns). In addition, as the rmsd time evolutions in Figure S2 show, structural changes can occur even at later times.

Compared to the native β CD, the peak of the rmsd distribution for β CD derivatives moves to higher values in all solvents except ME β CDs in water. For 2,6-ET β CD, the positions of the peaks were in the same range with the native β CD although their relative positions changed. For ME β CDs (Figures 2(b)-(e)), the lowest rmsd was found in non-polar solvents similar to the native β CD. The mono-substituted 2-ME β CD and 6-ME β CD showed large rmsd in OCT, while the rmsd of the di-substituted 2,6-DM β CD in CHX and OCT were similar. When the native β CD and ME β CDs were solvated in polar solvents, rmsd was increased. Moreover, structural change in WAT was less than in MeOH with the exception of 2-ME β CD. The fully substituted 2,3,6-TM β CD showed an increase in rmsd of 0.20-0.35 nm without any significant structural changes in different solvents.

In the case of the HP β CD derivatives, the long chain functional groups of 2-hydroxypropyl induced larger change in the rmsd compared to the other β CD types. The rmsds of the 2-HP β CD and 2,6-HP β CD were small in CHX and large in polar solvents, the largest in OCT for 2-HP β CD and in MeOH for 2,6-HP β CD. Similarly to 2,3,6-TM β CD, the structure of 6-HP β CD was relatively insensitive to the type of solvent. The peak of the rmsd of 6-HP β CD was in the range of 0.26-0.30 nm.

Finally, the hydrophobic 2,6-ET β CD was most unchanged in OCT. The structure underwent larger changes in CHX and polar solvents. The rmsds of the 2,6-ET β CD in WAT and MeOH were similar.

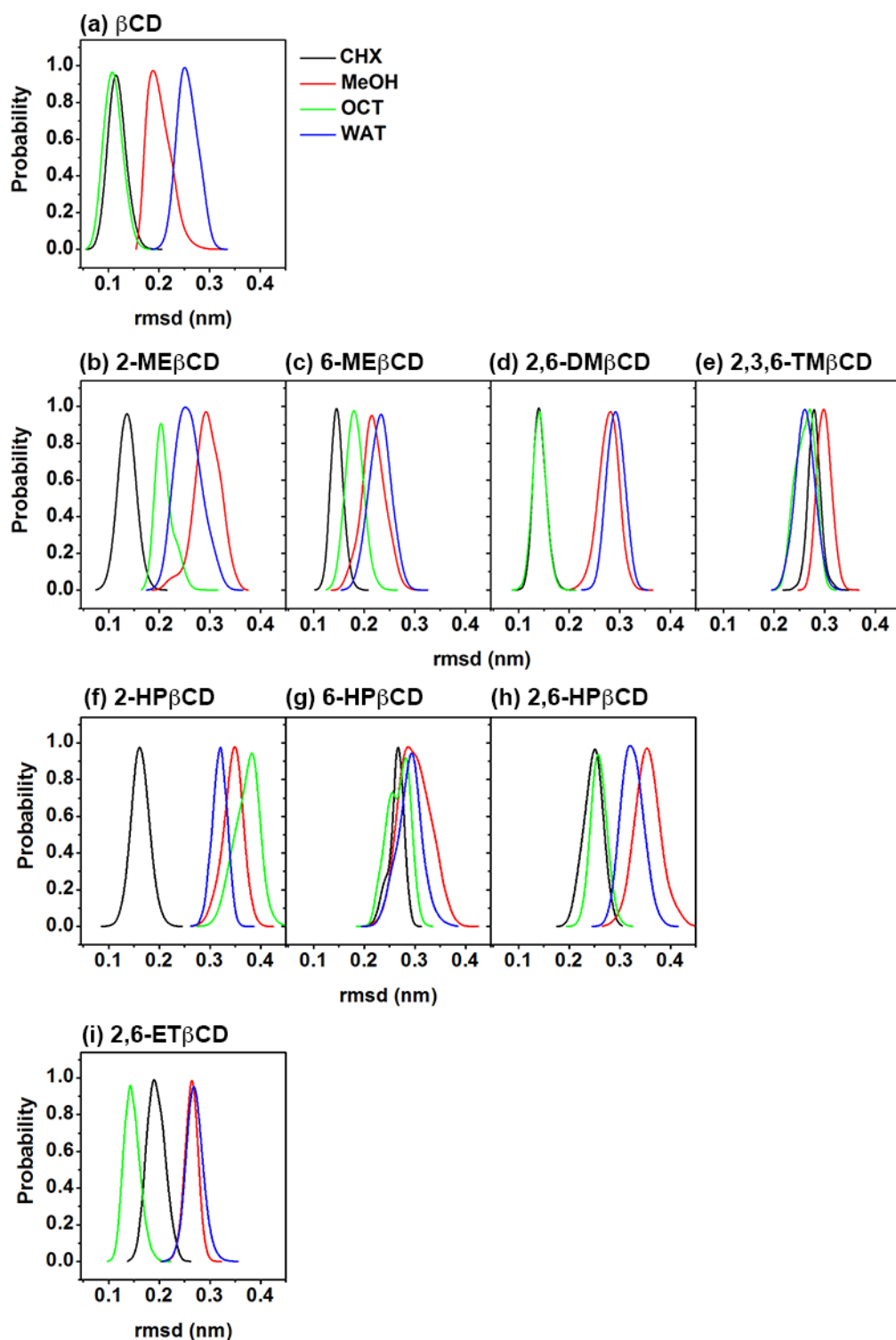


Figure 2: (a)-(i) The root mean square displacement (rmsd) distribution of the nine different β CDs in different solvents: CHX (black), MeOH (red), OCT (green) and WAT (blue). The polar solvents MeOH

and WAT induced larger structural changes in β CD derivatives with the exceptions of 2,3,6-TM β CD, 2-HP β CD and 6-HP β CD.

The root mean square fluctuations (rmsf) of atomic positions with respect to their initial coordinates were investigated (Figure 3(a)-(i)). The rmsf of each atom was averaged for the seven repeating glucose subunits, see atom labeling in Figure 1. The qualitative features of the rmsf profiles are the same in all systems with the exception of 2-HP β CD (Figure 3(f)) in which the middle peak is the highest one. In particular, the functional groups at the primary rim (at C6) exhibit more pronounced fluctuations compared to the functional groups at the secondary rim (at C2 and C3). In contrast, for 2-HP β CD (Figure 3(f)) large fluctuations were observed at the secondary rim at C2 functional groups.

Figure 3(a) shows that the native β CD exhibits less fluctuations in non-polar solvents. Compared to the β CD in WAT, the β CD in MeOH showed smaller fluctuations. This is in agreement with the previous simulations of Zhang et al.⁵⁸ Similarly, the ME β CD derivatives exhibit small fluctuations in non-polar solvents and increased rmsf in polar solvents. The difference between the rmsf in non-polar and polar solvents is shown for 6-ME β CD and 2,6-DM β CD (Figures 3(c) and 3(d)). For all ME β CD derivatives, 2-ME β CD displayed largest fluctuations. Among all the three HP β CD derivatives, 2-HP β CD has the smallest rmsf. The rmsf of 2-HP β CD has smallest fluctuations in WAT and fluctuations increase in CHX, MeOH and OCT.

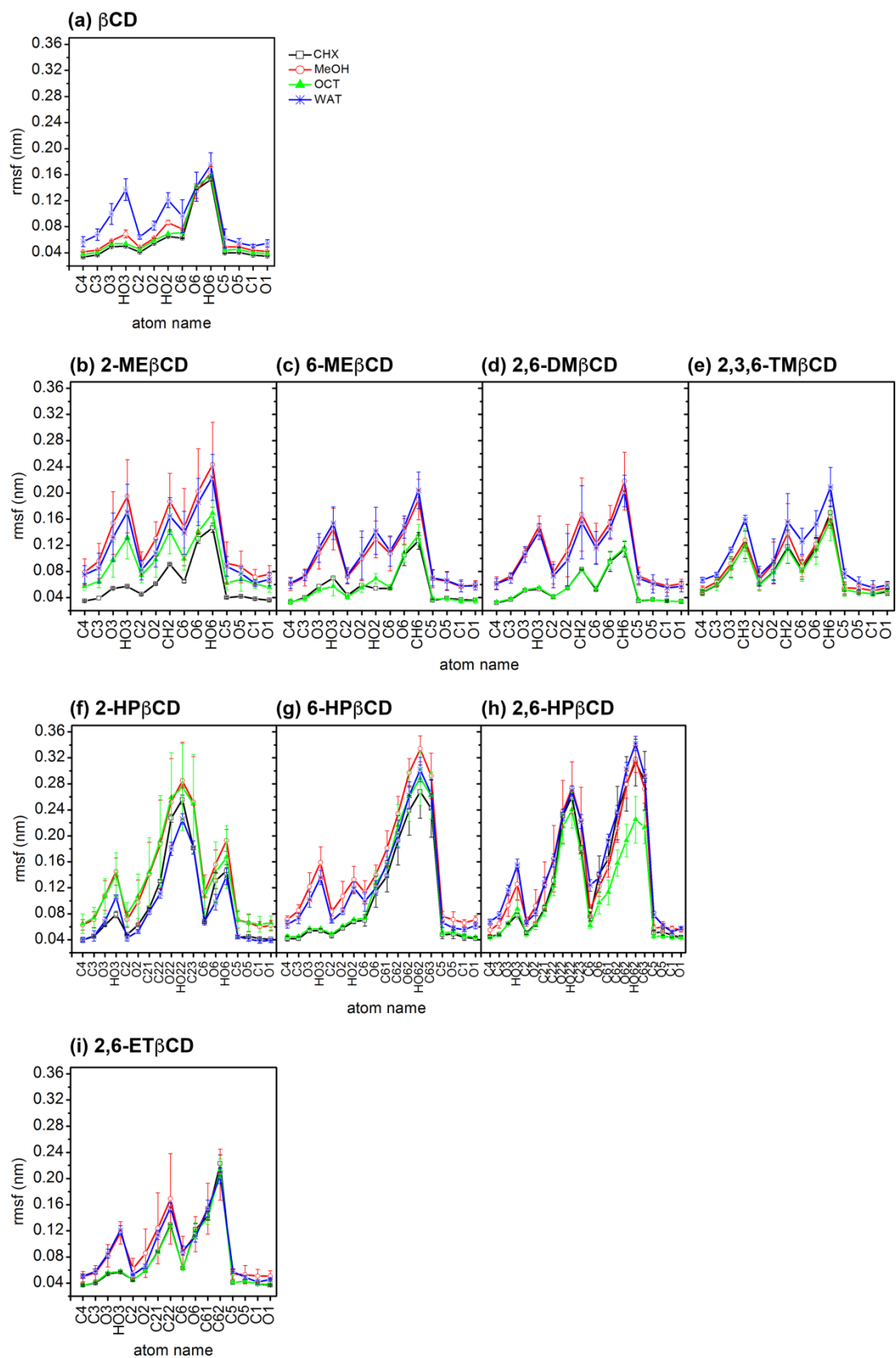


Figure 3: (a)-(i) The averages of root mean square fluctuations (rmsf) of the nine different β CDs in different solvents; CHX (black), MeOH (red), OCT (green) and WAT (blue), the higher fluctuation of β CDs structure was mostly found in polar solvents (WAT and MeOH), compared to non-polar solvents (OCT and CHX). Only the 2-HP β CD was more stable in WAT.

3.2) Hydrogen bonding

In addition, the number of intramolecular hydrogen bonds (H-bond) may have a significant impact on the structural stability of β CDs.⁵⁹⁻⁶¹ The number of hydrogen bonds between the -OR₁ group and the -OR₂ group of the adjacent glucose subunits was monitored in each of the cases. As detailed in Figure 4(a), the native β CD formed on average about 7 intramolecular H-bonds in both of the non-polar solvents, while only few hydrogen bonds were found in polar solvents. Being solvated in CHX, the number of adjacent H-bonds of the -OR₁ and -OR₂ groups for the native β CD were the same as for the β CD derivatives. There is an exception, however: for 2-HP β CD and 2,6-HP β CD, the number of adjacent H-bonds for the -OR₁ and -OR₂ groups are higher than for the native β CD. In OCT, the number of adjacent H-bonds was in the same range as in CHX, except for 2-ME β CD and 2-HP β CD. These results correspond to the comparison of structural changes in CHX and OCT. In polar solvents, the adjacent H-bond for the native β CD was smaller than for the β CD derivatives, especially in MeOH. The loss of intramolecular H-bonds of β CDs resulted from increased intermolecular H-bonding between the β CDs and polar solvents (Table 2). Similar effects were seen in all β CD derivatives albeit with some interesting characteristics that will be discussed in the next section in connection with the shape analysis.

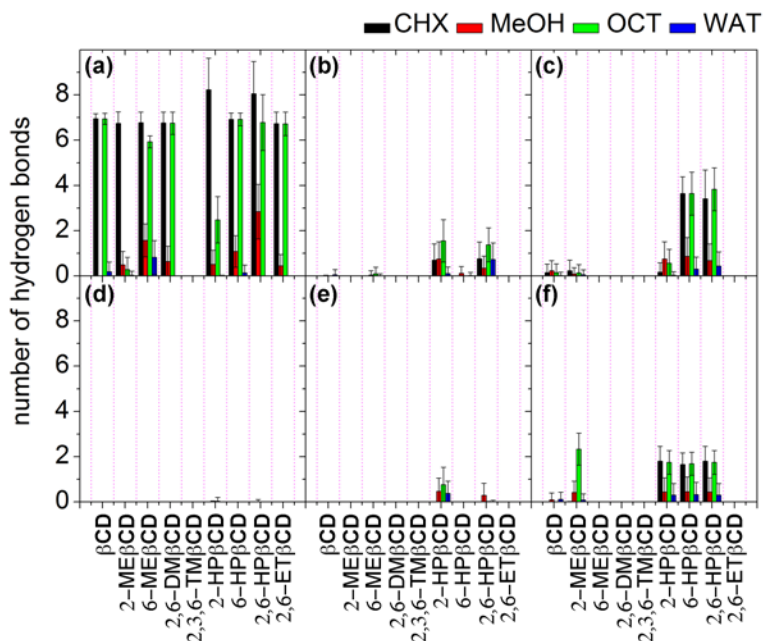


Figure 4: (a)-(c) intramolecular hydrogen bonds between the adjacent glucose subunits (shown in Figure 1): (a) the -OR₁ and -OR₂ groups, (b) the -OR₁ and -OR₁ groups, and (c) the -OR₃ and -OR₃ groups. Figures (d)-(f) show intramolecular hydrogen bonds between the non-adjacent glucose subunits: (d) the -OR₁ and -OR₂ groups, (e) the -OR₁ and -OR₁ groups, and (f) the -OR₃ and -OR₃ groups. There are no hydrogen donors or acceptors in 2,3,6-TM β CD.

Table 2: The number of hydrogen bonds between the β CDs and polar solvents. Error is given as standard deviation.

System	Average numbers of H-bonds	
	MeOH	WAT
β CD	32.8 \pm 3.0	42.3 \pm 3.1
2-ME β CD	22.3 \pm 2.8	34.0 \pm 2.9
6-ME β CD	21.9 \pm 2.8	32.3 \pm 3.0
2,6-DM β CD	15.2 \pm 2.3	25.0 \pm 2.5
2,3,6-TM β CD	6.9 \pm 1.8	15.2 \pm 2.4
2-HP β CD	29.1 \pm 3.3	45.1 \pm 3.3
6-HP β CD	30.9 \pm 3.5	44.2 \pm 3.4
2,6-HP β CD	30.1 \pm 3.4	47.0 \pm 3.8
2,6-ET β CD	14.8 \pm 2.3	23.7 \pm 2.5

Our results suggest that non-polar solvents (CHX and OCT) may stabilize the structures for most of the β CDs except for 2-HP β CD in OCT. The deformation of 2-HP β CD in OCT could be found because some substituent flipped toward inside the cavity and interacted with their non-neighbor substituents (Figure S3). Moreover, the inclusion of the OCT inside the 2-HP β CD's cavity was not found, while the CHX could be bound to the cavity (Figure S3). The inclusion complex of non-polar solvents inside the β CDs' cavity may also play role in the β CDs structure stabilization. Interestingly, 2,6-ET β CD shows lesser structural changes in OCT as compared to the other β CD derivatives. Molecules of polar solvents, water and methanol, may be present inside the cavity interior as shown in Figures S4 and S5. Water molecules present inside the native β CD cavity were found similarly to the X-ray crystal structures^{62, 63}. For β CD derivatives, the number of water molecules inside the cavity of difunctionalized β CD derivatives was significantly higher than in monofunctionalized β CDs. A few methanol molecules were observed inside cavity, except for 2-ME β CD and 2-HP β CD. No methanol molecules were present inside the deformed cavity of those β CDs. Molecules of the polar solvents were located at the hydrogen acceptors and hydrogen donors of the β CDs, that is, not inside the cavity. Hydrogen bonds with polar solvents were formed resulting in structural deformation of β CDs. Polar solvents caused higher fluctuations in β CDs'

structures, especially for the native β CD and the ME β CD derivatives. The structural changes of β CDs as well as their shapes may be factors in altering guest ligands' binding to the cavity interior. The influence of solvents on the β CDs' shapes will be discussed in the next section.

3.3) Shape of β CDs

The radius of gyration (R_g) and asphericity (b) were examined to describe sizes and shapes. The three principal moments (λ_1 , λ_2 and λ_3 where $\lambda_1^2 \geq \lambda_2^2 \geq \lambda_3^2$) following the common ordering convention) of the R_g tensor were measured. R_g can be given in terms of the principal moments as $R_g = \sqrt{\lambda_1^2 + \lambda_2^2 + \lambda_3^2}$ and asphericity as $b = \lambda_1 - \frac{1}{2}(\lambda_2 + \lambda_3)$. For a spherically symmetric object $b = 0$.

To explore the local structural properties, the areas (A) of core structure (Figure 1) at each rim were calculated using

$$A = \frac{\pi}{7} \sum_{i=1}^7 r_i^2, \quad (1)$$

where r_i is the distance between the β CD's center and the group of atoms of interest in glucose subunit i . The β CD's center was determined as the center of mass (COM) of all O1 atoms. The groups of interest are: 1) O1 atoms, 2) C6...O6...R₃ groups, and 3) O2...R₁ groups in glucose subunits. They were used to represent the cavity area at the core structure (A_{core}), the primary rim (A_1) and the secondary rim (A_2), respectively. The definitions of areas are shown in Figure 1.

The averages of R_g and b are shown in Table 3. The time evolutions of R_g and its three principal components (λ_1 , λ_2 and λ_3) are plotted in Figure S6. Additionally, snapshots from the final configurations at $t=100$ ns are shown in Figure 5. As compared to the native β CD, the R_g are in the same range (0.61-0.65 nm) for the ME β CD and increased for HP β CD and ET β CD. The increase of R_g in water is in quantitative agreement with previous simulations of β CD and HP β CD.²² For the different solvents, the R_g s do not show significant differences. Circularity can be examined by using the three principal components; when two of the principal components are equal, the planar structure is circular, the smallest value is in the direction along the cylindrical axis. Their time evolutions (Figure S6) suggest that the native β CD is very close to circular with the exception of water solution where the two largest principal components attain different values after about 10 ns. Regarding all derivatives, the highest degree of circularity is observed in CHX. As Figure S6 also shows, it is clear that long simulations times are needed to capture structural changes. In addition, in polar solvents (MeOH and WAT) the native β CD showed higher asphericity than in non-polar solvents by 22% and 56%, respectively (in Table 2). For the ME β CD

derivatives in non-polar solvents, the cavity mostly formed a circular shape with the exception of 2,3,6-TM β CD. The 12-38% difference in λ_1 and λ_2 for 2,3,6-TM β CD in all solvents indicates the cavity to be ellipsoidal. This is an agreement with X-ray studies.¹⁹ Compared to solvation in CHX, solvation in MeOH showed increasing asphericity by 62%, 50% and 68% for 2-ME β CD, 6-ME β CD and 2,6-DM β CD, respectively. In the case of the HP β CD derivatives, most of the HP β CDs in non-polar solvents had an approximately spherical cavity. In contrast, the HP β CD cavity in polar solvents was elliptical: large differences between λ_1 and λ_2 values, in the range of 8-37%, were found, especially for 2-HP β CD in MeOH (37%) and OCT (32%). In the case of the di-substituted 2,6-HP β CD, λ_1 and λ_2 showed no significant dependence on the type of solvent. However, λ_3 increased to be in the same range with λ_1 and λ_2 especially when the 2,6-HP β CD was solvated by WAT. The HP β CD derivatives with substitutions at both 2- and 6-positions were more spherical than the substitutions at only one of those positions. This is in agreement with the simulations of HP β CD derivatives in water.²² Most of the HP β CDs in CHX were more spherical than in the other solvents; the 2,6-HP β CD in WAT has the lowest asphericity. The spherical shape was highly deformed in OCT and in MeOH in case of 2-HP β CD and the change occurred after a significant time (Figure S6). Finally, in case of the 2,6-ET β CD, λ_1 and λ_2 fluctuated in the same range independent of the type of solvent. It indicates that the circular cavity of 2,6-ET β CD was maintained in all solvents. The λ_3 of the 2,6-ET β CD in CHX and OCT were similar. By comparing in CHX, the decrease of λ_3 was found by 19% and 10% when the 2,6-ET β CD was solvated by MeOH and WAT, respectively. Interestingly, the 2,6-ET β CD remained spherical in all solvents ($b \sim 0.08$ - 0.09).

Table 3: The effect of solvent on the radius of gyration (R_g) and asphericity (b). Most of the β CDs are larger and more spherical in non-polar solvents than in polar solvents. Errors are given in terms of standard deviation. The errors in R_g and b are less than 0.01 and 0.03, respectively.

System	Radius of gyration; R_g (nm)				Asphericity; b			
	CHX	MeOH	OCT	WAT	CHX	MeOH	OCT	WAT
β CD	0.62 \pm 0.01	0.62 \pm 0.01	0.62 \pm 0.01	0.60 \pm 0.01	0.09 \pm 0.01	0.11 \pm 0.01	0.09 \pm 0.01	0.14 \pm 0.02
2-ME β CD	0.64 \pm 0.01	0.61 \pm 0.01	0.60 \pm 0.01	0.62 \pm 0.01	0.09 \pm 0.01	0.15 \pm 0.02	0.10 \pm 0.01	0.13 \pm 0.02
6-ME β CD	0.62 \pm 0.01	0.62 \pm 0.01	0.61 \pm 0.01	0.61 \pm 0.01	0.08 \pm 0.01	0.12 \pm 0.02	0.09 \pm 0.01	0.12 \pm 0.02
2,6-DM β CD	0.64 \pm 0.01	0.62 \pm 0.01	0.64 \pm 0.01	0.62 \pm 0.01	0.08 \pm 0.01	0.13 \pm 0.02	0.08 \pm 0.01	0.10 \pm 0.02
TM β CD	0.63 \pm 0.01	0.63 \pm 0.01	0.63 \pm 0.01	0.65 \pm 0.01	0.13 \pm 0.01	0.14 \pm 0.01	0.15 \pm 0.01	0.11 \pm 0.01
2-HP β CD	0.70 \pm 0.01	0.66 \pm 0.01	0.65 \pm 0.01	0.66 \pm 0.01	0.10 \pm 0.01	0.16 \pm 0.02	0.14 \pm 0.02	0.10 \pm 0.01
6-HP β CD	0.64 \pm 0.01	0.66 \pm 0.01	0.64 \pm 0.01	0.65 \pm 0.01	0.09 \pm 0.02	0.12 \pm 0.03	0.09 \pm 0.02	0.12 \pm 0.03
2,6-HP β CD	0.72 \pm 0.01	0.72 \pm 0.01	0.71 \pm 0.01	0.69 \pm 0.01	0.08 \pm 0.02	0.11 \pm 0.02	0.08 \pm 0.02	0.06 \pm 0.01
2,6-ET β CD	0.67 \pm 0.01	0.65 \pm 0.01	0.67 \pm 0.01	0.64 \pm 0.01	0.08 \pm 0.01	0.09 \pm 0.01	0.08 \pm 0.01	0.09 \pm 0.01

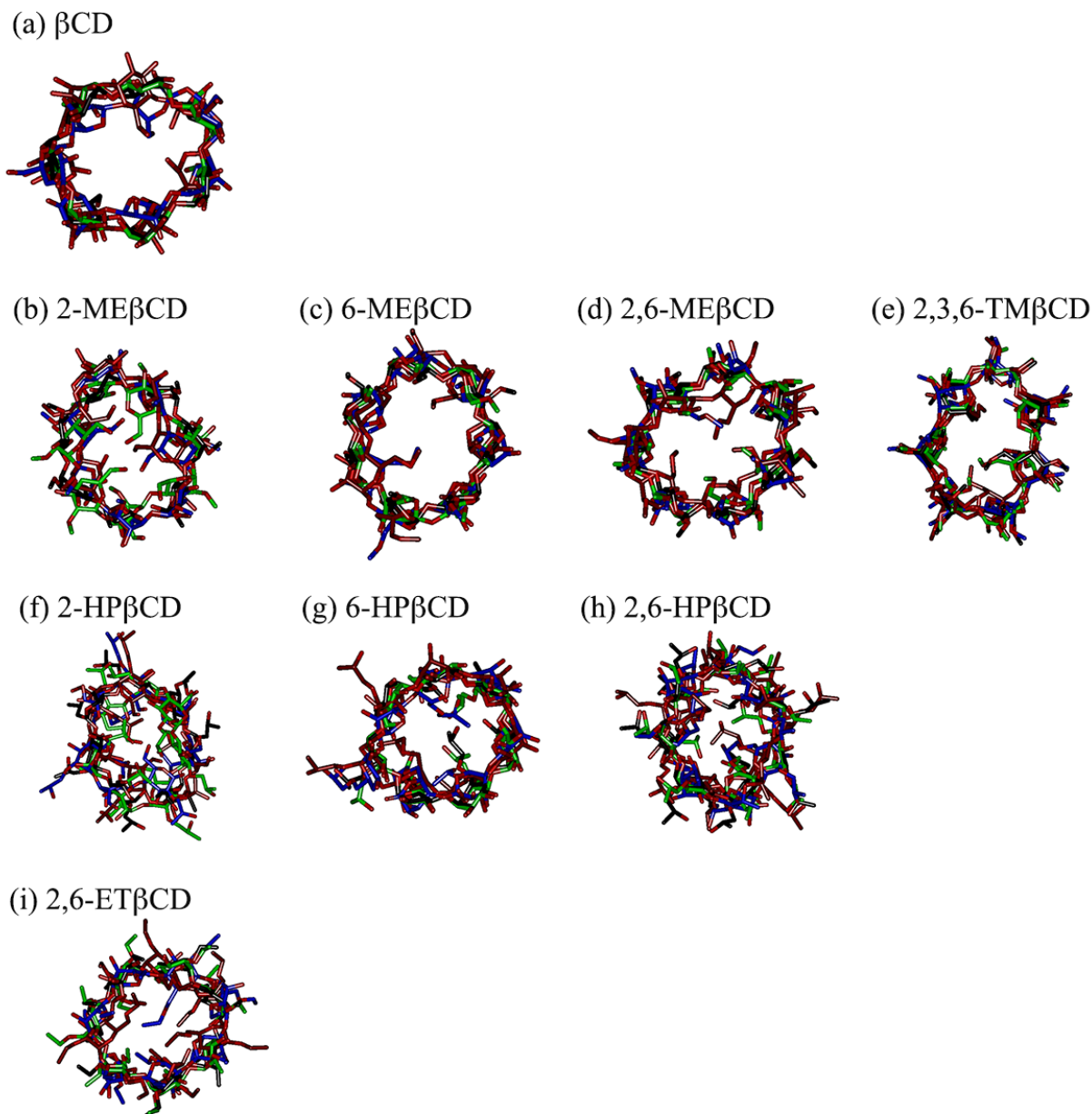


Figure 5: Superposition of the last MD snapshot of each β CD type in different solvents, the native β CD and β CD derivatives in CHX, MeOH, OCT and WAT are represented by the black-, red-, green- and blue-stick, respectively. The cyclic drastic deformation was found in polar solvents, especially for the 2,3,6-TM β CD, 2-HP β CD and 2,6-HP β CD.

The cavity areas of the core structure (A_{core}), the primary rim (A_1) and the secondary rim (A_2) are shown in Figures 6(a)-(i), the definitions for the areas are provided in Figure 1. The results show that for all β CD types, A_{core} does not depend significantly on solvent type. At the rims, the area A_2 was more

influenced by the solvent type than A_1 . For the native β CD, the A_2 was larger than A_1 in non-polar solvents. In contrast, the area at the primary rim was larger than at the secondary rim in polar solvents. Solvation of the native β CD in MeOH leads to a narrow secondary rim.

For the ME β CD derivatives (Figure 6(b)-(e)), cavity sizes show dependence on functionalization. In non-polar solvents, A_2 of the 2-ME β CD and 2,6-DM β CD increased to $\sim 1.8 \text{ nm}^2$ whereas the native β CD and the rest of the ME β CD derivatives had $A_2 \sim 1.4 \text{ nm}^2$. Relatively open secondary rims were found in non-polar solvents for 2-ME β CD and 2,6-DM β CD, compared to their primary rims. In polar solvents, however, A_1 and A_2 were similar for most of the ME β CD derivatives.

Figure 6(e) shows that there is no solvent effect on the TM β CD cavity size. In case of the HP β CD derivatives (Figure 6(f)-(h)), the area of substituted rim was larger than the rim without functional groups. Functionalization with long chain of 2-hydroxypropyl resulted in large areas compared to the native β CD and the other β CD derivatives. The areas at all parts of 2-HP β CD did not show any dependence on the type of solvent and 2-HP β CD had its secondary rim more open than the primary. In contrast, the primary rim of 6-HP β CD was more opened in all solvents. When both rims had substitutions, A_2 of 2,6-HP β CD was larger than A_1 in most of the solvents. The only exception was water. For 2,6-ET β CD, the secondary rim was larger in non-polar solvents and A_1 was equal to A_2 in polar solvents.

Shape analysis shows that β CDs in non-polar solvents have mostly spherical cavities whereas cavity deformations were found in polar solvents. The type of functionalization also had an influence on the cavity shape. Substitution at only one rim showed less circularity compared to the ME β CD and HP β CD with functional groups on their both rims. However, no significant changes in the area at the core (Figure 1) for different functional groups were observed. However, among the three functional groups, substitution with hydroxypropyl showed slightly larger area at the rims, especially at the rim(s) with the substituent.

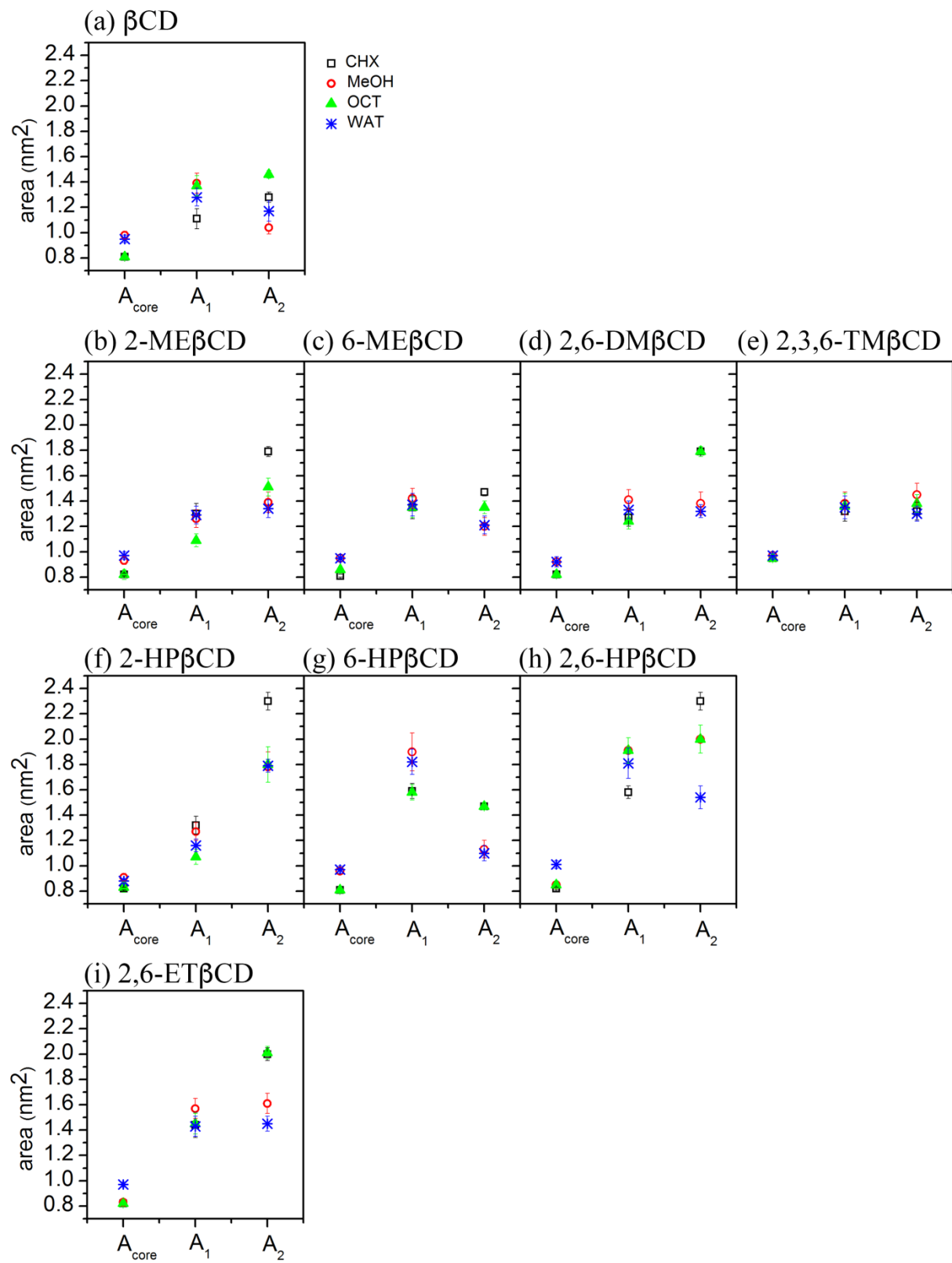


Figure 6: The area (Figure 1) at the core (A_{core}), the primary rim (A_1) and the secondary rim (A_2) in the presence of different solvents. There was no significant change in A_{core} with different solvents or functional groups. A_2 was mostly larger than A_1 in non-polar solvents.

Before leaving this section, we discuss the relation between principal components and intramolecular hydrogen bonding. The case of native β CD has already been addressed above and so we focus on the β CD derivatives. Comparison of the time evolution of the principal moments (Figure S6) and the number of hydrogen bonds between the different glucose subunits (Figure 4) reveals the stabilizing influence of H-bonds between the adjacent -OR1 and -OR2 groups (Figure S7(a)) on the secondary rim, and the destabilizing effect of the H-bonds between the -OR3 groups (Figure 4c,f). In particular, when H-bonds between the -OR3 groups exist, fluctuations in the principal moments (Figure S6) become very pronounced. That is exemplified by the behavior of all HP β CDs. 2,3,6-TM β CD is another special case as it does not have any intramolecular H-bonds and it also shows large fluctuations. Side and top views of few of the cases are shown in Figure S7.

3.4) Solvation free energies

Solvation free energies ($G_{solvation}$) were estimated using the Molecular Mechanic/Poisson-Boltzmann Surface Area (MM/PBSA) method.⁶⁴ $G_{solvation}$ is the free energy difference between the solute in solvent and vacuum. It is composed of contributions due to electrostatic (G_{polar}) and non-electrostatic ($G_{non-polar}$) terms. G_{polar} is estimated using a Poisson-Boltzmann model. The dielectric constant of the β CDs molecule was set to be equal to one.⁶⁵ The dielectric constants of the solvents were extracted from experiments.⁶⁶ The non-polar contribution depends on the β CD's geometry. The MM/PBSA calculation was performed at the rate of every 1 ns for the last 30 ns of MD trajectory. We would like to mention issues. First, MM/PBSA is a so-called end-point method, that is, only the free energy difference between two states is considered. Thus, it does not take entropic contributions fully into account. A recent review of free energy methods discussing MM/PBSA and alternatives is provided by Hansen and van Gunsteren.⁶⁷ The second issue is that solubility is not determined by solvation free energy alone. To properly account for solvation, the free energy of the solid phase should also be taken into account. A recent review is provided by Skyner et al..⁶⁸

The average $G_{solvation}$, and the components G_{polar} and $G_{non-polar}$ are shown in Figure 7. The main contribution to the free energy was observed to be always due to the polar interactions. The non-polar contribution in all cases constituted less than 30% of the total solvation free energy. The lowest non-polar

contribution in water was found for the native β CD, followed by 6-ME β CD, 2-ME β CD, 2,6-DM β CD, 6-HP β CD, 2-HP β CD, TM β CD, 2,6-ET β CD and 2,6-HP β CD, respectively. The results in Figure 7 suggest that all β CDs favor polar solvents. In bulk water, the order for $G_{\text{solvation}}$ was TM β CD > 2,6-ET β CD > 2,6-DM β CD > 6-ME β CD > 2-ME β CD > β CD > 2-HP β CD ~ 6-HP β CD > 2,6-HP β CD. This order correlates well with hydrogen bonding (Table 2). The solvation free energies are qualitative agreement with experiments using the HP β CD and ET β CD derivatives.^{26, 30}

In MeOH, $G_{\text{solvation}}$ is higher compared to water. The same trend as in water was observed with one exception: there was no significant difference in $G_{\text{solvation}}$ between the HP β CD derivatives. In non-polar solvents, $G_{\text{solvation}}$ was observed to be about five times higher than in polar solvents. TM β CD has the highest $G_{\text{solvation}}$ in CHX, followed by the 2,6-ET β CD, 2,6-DM β CD, 6-ME β CD, 6-HP β CD, 2,6-HP β CD, 2-ME β CD, β CD and 2-HP β CD. The order is the same in OCT.

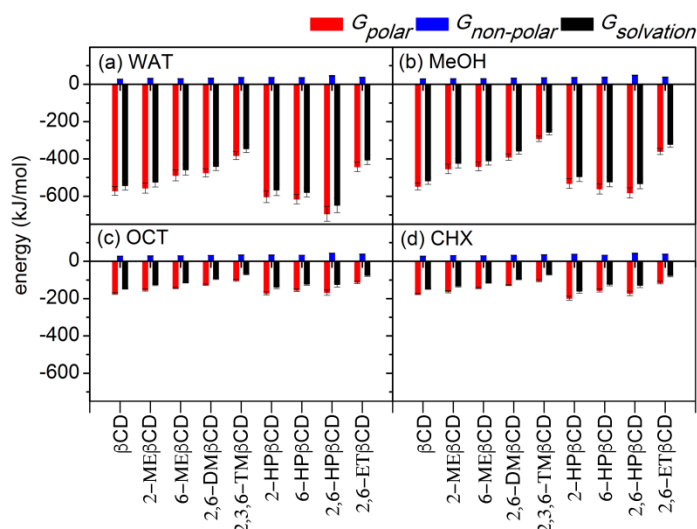


Figure 7: Solvation free energy, $G_{\text{solvation}}$ (black), and contributions from polar (red) and non-polar (blue) interactions. For the same type of β CD, $G_{\text{solvation}}$ was always lowest in WAT, followed by MeOH and non-polar solvents, respectively.

4. Conclusions

In the present work, conformational properties of the native β CD and eight of its derivatives, both hydrophilic and hydrophobic types, in four different solvents were investigated by MD simulations. Our results show that the polar solvents have strong influence on the structural stability of β CDs: intramolecular hydrogen bonds were lost, resulting in deformation of the β CDs' ring and decreased

structural stability. An interesting exception to this behavior was solvation in octane which induced less stability and significant changes in the 2-HP β CD structure.

Interestingly, the hydrophobic 2,6-ET β CD structure showed high rigidity and the spherical shape of the cavity remained intact in all solvents. We propose that this high stability, which correlates well with its high ligand-binding affinity, may be the reason why 2,6-ET β CD can act as a sustained release drug carrier. The effect of polar solvents on the other β CD types was very different and both the positions and number of functional groups influenced their shape. In the case of di-substitution at C2 and C6, ME β CDs and HP β CDs had spherical cavity, while the mono-substituted ones had elliptical cavities. In addition, in non-polar solvents the secondary rim (Figure 1) remained relatively open while it was narrowed in polar solvents. The long chain of 2-hydroxypropyl functional groups of the HP β CD derivatives resulted in larger areas (Figure 1), especially at the substituted rim. The MM/PBSA calculations showed that the solvation free energy of each β CDs type was different depending on their chemical functional groups and the numbers of the substituent groups. All β CDs preferred solvation by polar solvents. In general, the atomistic details of the conformations in various solvents are highly useful for the selection of the appropriate β CDs in pharmaceutical applications and other applications, and in the development in drug delivery systems.

ASSOCIATED CONTENT

Supporting Information

The Supporting Information is available free of charge.

Notes

The authors declare no competing financial interest.

Acknowledgements

This work was financially supported by Kasetsart University Research and Development Institute (KURDI) and Faculty of Science at Kasetsart University (JW), and Natural Sciences and Engineering Research Council of Canada (MK).

References

1. M. P. di Cagno, *Molecules*, 2016, **22**, 1-14
2. G. Astray, C. Gonzalez-Barreiro, J. C. Mejuto, R. Rial-Otero and J. Simal-Gándara, *Food Hydrocoll.*, 2009, **23**, 1631-1640.
3. Our ingredients: See what Febreze is made of, <http://www.febreze.com/en-us/learn/febreze-ingredients>. , (accessed 1 May, 2017).

4. G. Crini, *Chem. Rev.*, 2014, **114**, 10940-10975.
5. K. Uekama, N. Hirashima, Y. Horiuchi, F. Hirayama, T. Ijitsu and M. Ueno, *J. Pharm. Sci.*, 1987, **76**, 660-661.
6. V. J. Stella and Q. He, *Toxicol. Pathol.*, 2008, **36**, 30-42.
7. D. W. Frank, J. E. Gray and R. N. Weaver, *Am. J. Pathol.*, 1976, **83**, 367-382.
8. L. Szente and J. Szejtli, *Adv. Drug Delivery Rev.*, 1999, **36**, 17-28.
9. J. Deng, X. Liu, S. Zhang, C. Cheng, C. Nie and C. Zhao, *Langmuir*, 2015, **31**, 9665-9674.
10. J. Qiu, L. Kong, X. Cao, A. Li, H. Tan and X. Shi, *RSC Adv.*, 2016, **6**, 25633-25640.
11. C. Jullian, M. Alfaro, G. Zapata-Torres and C. Olea-Azar, *J. Solution Chem.*, 2010, **39**, 1168-1177.
12. C. Jullian, *J. Chil. Chem. Soc.*, 2009, **54**, 201-203.
13. M. Cirri, F. Maestrelli, S. Orlandini, S. Furlanetto, S. Pinzauti and P. Mura, *J. Pharm. Biomed. Anal.*, 2005, **37**, 995-1002.
14. D. Leonardi, M. E. Bombardiere and C. J. Salomon, *Int. J. Biol. Macromol.*, 2013, **62**, 543-548.
15. M. Okawara, F. Hashimoto, H. Todo, K. Sugibayashi and Y. Tokudome, *Int. J. Pharm.*, 2014, **472**, 257-261.
16. G. O. K. Loh, Y. T. F. Tan and K.-K. Peh, *Asian J. Pharm. Sci.*, 2016, **11**, 536-546.
17. M. Shah, V. Shah, A. Ghosh, Z. Zhang and T. Minko, *J. Pharm. Pharmacol.*, 2015, **2**, 1-17.
18. K. Harata, C. T. Rao, J. Pitha, K. Fukunaga and K. Uekama, *Carbohydr. Res.*, 1991, **222**, 37-45.
19. K. Harata, F. Hirayama, H. Arima, K. Uekama and T. Miyaji, *J. Chem. Soc., Perkin Trans. 2*, 1992, 1159-1166.
20. K. Harata, C. T. Rao and J. Pitha, *Carbohydr. Res.*, 1993, **247**, 83-98.
21. K. S. Boonyarattanakalin, P. Wolschann and L. Lawtrakul, *J. Inclusion Phenom. Macrocyclic Chem.*, 2011, **70**, 279-290.
22. C. W. Yong, C. Washington and W. Smith, *Pharm. Res.*, 2008, **25**, 1092-1099.
23. J. Y. Li, D. F. Sun, A. Y. Hao, H. Y. Sun and J. Shen, *Carbohydr. Res.*, 2010, **345**, 685-688.
24. T. Steiner, A. M. M. da Silva, J. J. C. Teixeira-Dias, J. Müller and W. Saenger, *Angew. Chem., Int. Ed. Engl.*, 1995, **34**, 1452-1453.
25. M. Jana and S. Bandyopadhyay, *J. Chem. Phys.*, 2011, **134**, 025103.
26. T. Loftsson, P. Jarho, M. Masson and T. Jarvinen, *Expert Opin. Drug Delivery*, 2005, **2**, 335-351.
27. D. Duchêne, *Cyclodextrins and their industrial uses*, Editions de santé, Paris, 1987.
28. A. K. Chatjigakis, C. Donze, A. W. Coleman and P. Cardot, *Anal. Chem.*, 1992, **64**, 1632-1634.
29. J. Szejtli, *Starch/Staerke*, 1984, **36**, 429-432.
30. V. Sinha, A. Nanda and R. Kumria, *Pharm. Technol.*, 2002, **26**, 36-47.

31. T. Kiss, F. Fenyvesi, N. Pasztor, P. Feher, J. Varadi, R. Kocsan, L. Szente, E. Fenyvesi, G. Szabo, M. Vecsernyes and I. Bacskay, *Pharmazie*, 2007, **62**, 557-558.
32. F. Hirayama and K. Uekama, *Adv. Drug Delivery Rev.*, 1999, **36**, 125-141.
33. L. Abdelmalek, M. Fatiha, N. Leila, C. Mouna, M. Nora and K. Djameleddine, *J. Mol. Liq.*, 2016, **224**, Part A, 62-71.
34. S. S. Jambhekar and P. Breen, *Drug Discov. Today*, 2016, **21**, 356-362.
35. S. Charumanee, S. Okonogi, J. Sirithunyalug, P. Wolschann and H. Viernstein, *Sci. Pharm.*, 2016, **84**, 694-704.
36. T. Kida, T. Iwamoto, Y. Fujino, N. Tohnai, M. Miyata and M. Akashi, *Org. Lett.*, 2011, **13**, 4570-4573.
37. F. C. Armbruster, in *Proceedings of the Fourth International Symposium on Cyclodextrins: Munich, West Germany, April 20–22, 1988*, Springer Netherlands, Dordrecht, 1988.
38. W. Snor, E. Liedl, P. Weiss-Greiler, A. Karpfen, H. Viernstein and P. Wolschann, *Chem. Phys. Lett.*, 2007, **441**, 159-162.
39. M. J. Abraham, T. Murtola, R. Schulz, S. Páll, J. C. Smith, B. Hess and E. Lindahl, *SoftwareX*, 2015, **1–2**, 19-25.
40. R. D. Lins and P. H. Hunenberger, *J. Comput. Chem.*, 2005, **26**, 1400-1412.
41. C. A. López, A. H. de Vries and S. J. Marrink, *PLoS Comput. Biol.*, 2011, **7**, e1002020.
42. J. Kicuntod, W. Khuntawee, P. Wolschann, P. Pongsawasdi, W. Chavasiri, N. Kungwan and T. Rungrotmongkol, *J. Mol. Graphics Modell.*, 2016, **63**, 91-98.
43. H. J. C. Berendsen, J. P. M. Postma, W. F. van Gunsteren and J. Hermans, in *Intermolecular Forces*, ed. B. Pullman, Reidel, Dordrecht, 1981, vol. 14, ch. 21, pp. 331-342.
44. T. Darden, D. York and L. Pedersen, *J. Chem. Phys.*, 1993, **98**, 10089-10092.
45. U. Essmann, L. Perera, M. L. Berkowitz, T. Darden, H. Lee and L. G. Pedersen, *J. Chem. Phys.*, 1995, **103**, 8577-8593.
46. M. Karttunen, J. Rottler, I. Vattulainen and C. Sagui, *Curr. Top. Membr.*, 2008, **60**, 49-89.
47. B. Hess, *J. Chem. Theory Comput.*, 2008, **4**, 116-122.
48. H. J. C. Berendsen, J. P. M. Postma, W. F. v. Gunsteren, A. DiNola and J. R. Haak, *J. Chem. Phys.*, 1984, **81**, 3684-3690.
49. G. Bussi, D. Donadio and M. Parrinello, *J. Chem. Phys.*, 2007, **126**, 014101.
50. G. Bussi, T. Zykova-Timan and M. Parrinello, *J. Chem. Phys.*, 2009, **130**, 074101.
51. P. Boonnoy, M. Karttunen and J. Wong-ekkabut, *Phys. Chem. Chem. Phys.*, 2017, **19**, 5699-5704.
52. E. A. Cino, W. Y. Choy and M. Karttunen, *J. Phys. Chem. B*, 2016, **120**, 1060-1068.
53. E. A. Cino, W. Y. Choy and M. Karttunen, *J. Chem. Theory Comput.*, 2012, **8**, 2725-2740.

54. J. Wong-Ekkabut and M. Karttunen, *J. Chem. Theory Comput.*, 2012, **8**, 2905-2911.
55. W. Humphrey, A. Dalke and K. Schulten, *J. Mol. Graphics*, 1996, **14**, 33-38.
56. E. Mixcoha, J. Campos-Terán and Á. Piñeiro, *J. Phys. Chem. B*, 2014, **118**, 6999-7011.
57. W. Khuntawee, P. Wolschann, T. Rungrotmongkol, J. Wong-ekkabut and S. Hannongbua, *J. Chem. Inf. Model.*, 2015, **55**, 1894-1902.
58. H. Y. Zhang, C. L. Ge, D. van der Spoel, W. Feng and T. W. Tan, *J. Phys. Chem. B*, 2012, **116**, 3880-3889.
59. K. Chacko and W. Saenger, *J. Am. Chem. Soc.*, 1981, **103**, 1708-1715.
60. H. Dodziuk, in *Cyclodextrins and Their Complexes*, Wiley-VCH Verlag GmbH & Co. KGaA, Weinheim, 2006, pp. 1-30.
61. M. M. Deshmukh, L. J. Bartolotti and S. R. Gadre, *J. Comput. Chem.*, 2011, **32**, 2996-3004.
62. T. Steiner and G. Koellner, *J. Am. Chem. Soc.*, 1994, **116**, 5122-5128.
63. B. Ivanova and M. Spiteller, *Int. J. Biol. Macromol.*, 2014, **64**, 383-391.
64. R. Kumari, R. Kumar and A. Lynn, *J. Chem. Inf. Model.*, 2014, **54**, 1951-1962.
65. Y. Choi and S. Jung, *Carbohydr. Res.*, 2004, **339**, 1961-1966.
66. A. A. Maryott and E. R. Smith, *Table of dielectric constants of pure liquids*, U.S. Govt. Print. Off., Washington, DC, 1951.
67. N. Hansen and W. F. van Gunsteren, *J. Chem. Theory Comput.*, 2014, **10**, 2632-2647.
68. R. E. Skyner, J. L. McDonagh, C. R. Groom, T. van Mourik and J. B. Mitchell, *Phys. Chem. Chem. Phys.*, 2015, **17**, 6174-6191.

